I S A V

Journal of Theoretical and Applied Vibration and Acoustics

journal homepage: http://tava.isav.ir

Free in-plane vibration of heterogeneous nanoplates using Ritz method

Shirko Faroughi *[,a], **Seyed Mohammad Hossein Goushegir** [b]

[a] *Assistant Professor, Faculty of Mechanical Engineerng, Urmia University of Technology, Urmia, Iran*

[b] *M.Sc. Student, Faculty of Mechanical Engineerng, Urmia University of Technology, Urmia, Iran*

KEYWORDS

Article history:
Received 08 September 2015

Received in revised form 27 October 2015

Accepted 05 December 2015

Available online 20 December 2015

Keywords:
In-plane vibration

Rectangular heterogeneous nanoplate

Nonlocal elasticity theory

Ritz method

ABSTRACT

In this paper, the Ritz method has been employed to analyze the free in-plane vibration of heterogeneous (non-uniform) rectangular nanoplates corresponding to Eringen's nonlocal elasticity theory. The non-uniformity is taken into account using combinations of linear and quadratic forms in the thickness, material density and Young's modulus. Two-dimensional boundary characteristic orthogonal polynomials are applied in the Ritz method in order to examine the nonlocal effect, aspect ratio, length of nanoplate and non-uniformity parameters on the vibrational behaviors of the nanoplate. Results are verified with the available published data and good agreements are observed. The outcomes confirm apparent dependency of in-plane frequency of nanoplate on the small scale effect, non-uniformity, aspect ratio and boundary conditions. For instance, frequency parameter decreases by increasing the nonlocal parameter in all vibration modes; the frequency parameters increase with length and aspect ratio of nanoplates. Furthermore, the effect of nonlocal parameters on the frequency parameter is more prominent at the higher aspect ratios. Finally, the effect of nonlocal parameter on the in-plane modes is also presented in this analysis.

1. Introduction

Nanomaterials have recently attracted much attention among the researchers of chemistry, physics and engineering due to their special mechanical, chemical, electrical, electronic and optical properties (Thomas and Aneesh, 2014 [1]). These special properties are obtained from their nanoscale dimensions (Murmu and Adhikari, 2010 [2]). Some examples of these nanomaterials are nanoclusters (Baletto and Ferrando, 2005 [3]), nano-balls, nano-fibers, nanorods (Afolabi et al., 2009 [4]), thin films, engineered surfaces, carbon nanotubes (CNTs), mono- and multi-layer graphene sheets (Nagashio et al., 2009 [5]). Nanoclusters, nanobeams and nanoplates have been considered as zero, one and two dimensional nanomaterials respectively

* Corresponding Author: Shirko Faroughi, Email: shirko@iust.ac.ir

(Gusev and Rempel , 2004 [6]). These excellent nanomaterials have numerous applications in the field of semiconductor devices, nano-actuators, atomic force microscope (AFM) tips, biological sensors, drug carriers, bio-probes and implants (Li et al., 2015 [7]).

In order to properly design nanostructures, their mechanical behavior should be thoroughly explored both experimentally and theoretically. Experimental analyses provide more accurate results, however, conducting experiments on nanoscale devices is extremely challenging, expensive and time consuming (Favero et al., 2009; Poot and Van der zant, 2008 [8, 9]). As a result, in the literature, many contributions have been focused on developing appropriate theoretical models to predict nanostructures' behaviors. Theoretical models are generally divided into three major categories: (i) atomistic modeling (Ball, 2001; Baughman et al., 2002 [10, 11]), (ii) hybrid atomistic-continuum mechanics (Bodily and Sun, 2003; Li and Chu, 2003 [12, 13]) and (iii) continuum models. Atomistic (discrete) and hybrid atomistic-continuum mechanics models such as molecular dynamics (MD) (Liu and Wang, 2015 [14]), molecular structural mechanics (MSM) (Li and Chu, 2005 [15]) and density functional theory (Yumura, 2011 [16]) require a large amount of computations and are not recommended for large-scale nanostructures. The third major category, continuum mechanics, includes classical (local) and non-classical (nonlocal) continuum approaches. The classical continuum approach cannot be used in modeling of nanostructures because of ignoring small-scale effects. Therefore, the non-classical continuum approaches have been widely applied to model nanostructures (Lu et al., 2006; Shen, 2011; Adali, 2012; Karamooz and Shahidi, 2013; Wang et al., 2011 [17-21]). This approach accounts for the effect of small-length scales (distance between individual atoms, surface properties and particle size) in studying the mechanical behavior of nanostructures. Nonlocal elasticity theory proposed by Eringen (1972, 1983 and 2002 [22-24]) has been widely employed for nanostructures among other nonlocal continuum mechanics. This theory states that the stress field corresponds to the strain tensor not only at a specific point, but also at the entire domain. Nonlocal elasticity theory has been employed to investigate the static, buckling, bending and free vibration behavior of nanorods (Chang, 2012 [25]), nanobeams (Loya et al., 2009 [26]), nanoplates (Aksencer and Aydogdu, 2011; Anjomanshoa, 2013 [27, 28]) and nanoshells (Hu et al., 2008 [29]).

In spite of the vast literature on free transverse vibration of nanobeams, nanoplates and nanoshells, few works have been dedicated to the nonlocal elasticity of free in-plane vibrations (FIV) for nanoplates (graphene sheets). In-plane modes of nanoplates (GSs) occur at high frequencies. However, flexural modes exhibit at lower frequencies and thus, they can be of very useful implication at high operating frequencies (Bansal and Lamon, 2015 [30]). Nanoplates employed in nanoelectromechanical resonators can be enormously excited and demonstrate in-plane modes (Yantchev and Katardjiev, 2013 [31]). In summary, it is necessary to obtain a comprehensive physical and mathematical understanding of the in-plane vibration of nanoplates.

The free in-plane vibration of nanoplates using nonlocal continuum mechanics is studied by Murmu and Pradhan (2009 [32]) and relations for the natural frequencies are derived using the separation of variables method. The effects of nonlocal parameter (scale coefficient) have been only investigated in their studies. Their computational approaches may not be generally applied to analyze FIV of nanoplates for all combinations of boundary conditions and non-uniform geometries of nanoplates. Non-uniform geometries of the nano-components must be taken into

account in order to efficiently design nanostructures (Cumings et al., 2000 [33]). This non-uniformity gives efficient vibration control in nano-sized structures (Brodsky, 2010 [34]).

To the best of authors' knowledge, the effects of non-uniformity on the in-plane vibration of nanoplates have not been previously presented based on any experimental and nonlocal continuum model. Therefore, in this paper, the effects of non-uniformity along with the small-scale effects on the FIV of nanoplates are presented. Here, the non-uniformity is considered using variable thickness, material density and Young's modulus. In this paper, the Ritz method, as an approximate numerical approach, is used to examine FIV of non-uniform nanoplates. The Ritz method has been previously employed for vibration analysis of nanobeams (Xu and Deng, 2014; Koochi et al., 2014; Chakraverty and Behera, 2015 [35-37]) and nanoplates (Chakraverty and Behera, 2014 [38]). In order to study the FIV of nanoplate, boundary characteristic orthogonal polynomials (BCOPs) (Bhat, 1985; Bhat, 1991; Dickinson and Diblasio, 1986; Singh and Chakraverty, 1994(a,b); Chihara, 1987; Gautschi et al., 1999 [39-45]) are applied in the Rayleigh-Ritz method. The BCOPs are generated through the Gram-Schmidt orthonormalization process. These polynomials used in the Ritz method carry out the process computationally efficient. This occurs because some entries of stiffness and mass matrices of the generalized eigenvalue problem become one and zero due to the orthonormality of the supposed shape functions. In this study, the effect of non-uniformity parameters, nonlocal parameter, boundary conditions, aspect ratio, length of nanoplate and mode number on the FIV of nanoplates are investigated. Moreover, the impact of small-scale effect on mode shapes of a non-uniform nanoplate is also presented.

2. Theoretical formulations

2.1. Theoretical formulation of nanoplate

A rectangular nanoplate with length and width a and b are considered as shown in Fig. 1. The origin point of the coordinate system is located at one corner of the nanoplate. The x and y axes are placed along the edges of the nanoplate and the z-axis is normal to the xy-plane as depicted in Fig. 1.

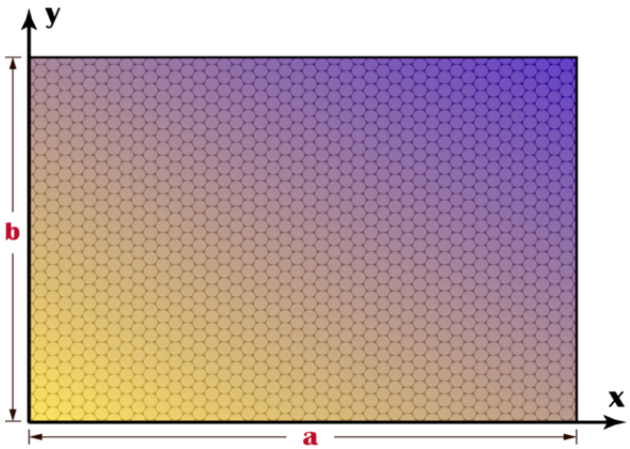

Fig. 1. A schematic of the nanoplate and the considered coordinate system

The nonlocal theory of elasticity considers that the stress at one point is a function of the strains at all other points in the body. Based on this assumption, the nonlocal constitutive relation for a Hookean solid is presented as follows (Lu et al., 2007 [46]):

$$\left(1 - e_0^2 {l_{in}}^2 \nabla^2\right)\sigma^{nl} = \sigma^l \tag{1}$$

where l_{in}, e_0 and ∇^2 denote an internal characteristic length, a constant for a specific material and the 2D Laplacian operator expressed in the Cartesian coordinate system $\nabla^2 = \left(\frac{\partial^2}{\partial x^2} + \frac{\partial^2}{\partial y^2}\right)$ respectively. Equation 1 can be written in the following two dimensional forms for FIV of nanoplates,

$$\begin{aligned}
\sigma_{xx} - e_0^2 {l_{in}}^2 \left(\frac{\partial^2 \sigma_{xx}}{\partial x^2} + \frac{\partial^2 \sigma_{xx}}{\partial y^2}\right) &= \frac{E(x,y)}{(1-\nu^2)}\left(\frac{\partial u}{\partial x} + \nu \frac{\partial v}{\partial y}\right), \\
\sigma_{yy} - e_0^2 {l_{in}}^2 \left(\frac{\partial^2 \sigma_{yy}}{\partial x^2} + \frac{\partial^2 \sigma_{yy}}{\partial y^2}\right) &= \frac{E(x,y)}{(1-\nu^2)}\left(\nu \frac{\partial u}{\partial x} + \frac{\partial v}{\partial y}\right) \\
\sigma_{xy} - e_0^2 {l_{in}}^2 \left(\frac{\partial^2 \sigma_{xy}}{\partial x^2} + \frac{\partial^2 \sigma_{xy}}{\partial y^2}\right) &= \frac{E(x,y)}{2(1+\nu)}\left(\frac{\partial u}{\partial y} + \frac{\partial v}{\partial x}\right)
\end{aligned} \tag{2}$$

where $E(x,y)$ and ν are the elastic modulus and Poisson's ratio of the non-uniform nanoplate respectively. Also, u and v denote the in-plane displacements along x and y directions, respectively. The equation of motion for FIV of plates can be written as (Gorman, 2004 [47]):

$$\begin{aligned}
\frac{\partial N_{xx}}{\partial x} + \frac{\partial N_{xy}}{\partial y} &= \rho(x,y) h \frac{\partial u^2}{\partial t^2} \\
\frac{\partial N_{yy}}{\partial y} + \frac{\partial N_{xy}}{\partial x} &= \rho(x,y) h \frac{\partial v^2}{\partial t^2}
\end{aligned} \tag{3}$$

where $\rho(x,y)$ and h denote the mass density and the thickness of the plate respectively and N_{xx}, N_{yy} and N_{xy} are the axial stress resultants expressed as:

$$N_{xx} = \int_{-h/2}^{h/2} \sigma_{xx}\, dz\ ,\ N_{yy} = \int_{-h/2}^{h/2} \sigma_{yy}\, dz,\ N_{xy} = \int_{-h/2}^{h/2} \sigma_{xy}\, dz \tag{4}$$

The above stress resultants are obtained by integrating Eq. 2 with respect to the thickness of the plate as follows:

$$\begin{aligned}
N_{xx} - e_0^2 {l_{in}}^2 \left(\frac{\partial^2 N_{xx}}{\partial x^2} + \frac{\partial^2 N_{xx}}{\partial y^2}\right) &= \frac{E(x,y)h}{(1-\nu^2)}\left(\frac{\partial u}{\partial x} + \nu \frac{\partial v}{\partial y}\right) \\
N_{yy} - e_0^2 {l_{in}}^2 \left(\frac{\partial^2 N_{yy}}{\partial x^2} + \frac{\partial^2 N_{yy}}{\partial y^2}\right) &= \frac{E(x,y)h}{(1-\nu^2)}\left(\nu \frac{\partial u}{\partial x} + \frac{\partial v}{\partial y}\right) \\
N_{xy} - e_0^2 {l_{in}}^2 \left(\frac{\partial^2 N_{xy}}{\partial x^2} + \frac{\partial^2 N_{xy}}{\partial y^2}\right) &= \frac{E(x,y)h}{2(1+\nu)}\left(\frac{\partial u}{\partial y} + \frac{\partial v}{\partial x}\right)
\end{aligned} \tag{5}$$

The governing equations of motion for FIV of non-uniform nanoplate in Cartesian coordinates can be obtained by substituting Eq. 5 into Eq. 3 as follows:

$$\frac{\partial}{\partial x}\left(\frac{E(x,y)h}{(1-\nu^2)}\left(\frac{\partial u}{\partial x}+\nu\frac{\partial v}{\partial y}\right)\right)+\frac{\partial}{\partial y}\left(\frac{E(x,y)h}{2(1+\nu)}\left(\frac{\partial u}{\partial y}+\frac{\partial v}{\partial x}\right)\right)-\rho(x,y)h\frac{\partial u^2}{\partial t^2}$$
$$+e_0^2 {l_{in}}^2\frac{\partial^2}{\partial x^2}\left(\rho(x,y)h\frac{\partial u^2}{\partial t^2}\right)+e_0^2 {l_{in}}^2\frac{\partial^2}{\partial y^2}\left(\rho(x,y)h\frac{\partial u^2}{\partial t^2}\right)=0, \tag{6-a}$$

$$\frac{\partial}{\partial y}\left(\frac{E(x,y)h}{(1-\nu^2)}\left(\nu\frac{\partial u}{\partial x}+\frac{\partial v}{\partial y}\right)\right)+\frac{\partial}{\partial x}\left(\frac{E(x,y)h}{2(1+\nu)}\left(\frac{\partial u}{\partial y}+\frac{\partial v}{\partial x}\right)\right)-\rho(x,y)h\frac{\partial v^2}{\partial t^2}$$
$$+e_0^2 {l_{in}}^2\frac{\partial^2}{\partial x^2}\left(\rho(x,y)h\frac{\partial v^2}{\partial t^2}\right)+e_0^2 {l_{in}}^2\frac{\partial^2}{\partial y^2}\left(\rho(x,y)h\frac{\partial v^2}{\partial t^2}\right)=0. \tag{6-b}$$

Equations (6-a) and (6-b) are the consistent basic equations for the FIV of non-uniform nanoplate model. These equations are reduced to the FIV equation of non-uniform local plate when $e_0 l_{in}=0$. Equations 6 are the strong form of the governing equations for the FIV of non-uniform nanoplate corresponding to the nonlocal elasticity theory. Owing to the fact that finding the exact solution for a strong form of FIV for non-uniform nanoplate is commonly difficult, a weak form of their equations is usually produced for the processes. Here, weighted residual method as a general mathematical tool is used in order to create the weak form of the governing equations of motion for the FIV of non-uniform nanoplate. Based on this approach, the weighted residual formulation of the equation of motion in Eqs. 6 is obtained as:

$$\iint_A \psi_u(x,y)\left(\frac{\partial}{\partial x}\left(\frac{E(x,y)h}{(1-\nu^2)}\left(\frac{\partial u}{\partial x}+\nu\frac{\partial v}{\partial y}\right)\right)+\frac{\partial}{\partial y}\left(\frac{E(x,y)h}{2(1+\nu)}\left(\frac{\partial u}{\partial y}+\frac{\partial v}{\partial x}\right)\right)-\rho(x,y)h\frac{\partial u^2}{\partial t^2}\right.$$
$$\left.+e_0^2 {l_{in}}^2\frac{\partial^2}{\partial x^2}\left(\rho(x,y)h\frac{\partial u^2}{\partial t^2}\right)+e_0^2 {l_{in}}^2\frac{\partial^2}{\partial y^2}\left(\rho(x,y)h\frac{\partial u^2}{\partial t^2}\right)\right)dxdy=0, \tag{7-a}$$

$$\iint_A \psi_v(x,y)\left(\frac{\partial}{\partial y}\left(\frac{E(x,y)h}{(1-\nu^2)}\left(\nu\frac{\partial u}{\partial x}+\frac{\partial v}{\partial y}\right)\right)+\frac{\partial}{\partial x}\left(\frac{E(x,y)h}{2(1+\nu)}\left(\frac{\partial u}{\partial y}+\frac{\partial v}{\partial x}\right)\right)-\rho(x,y)h\frac{\partial v^2}{\partial t^2}\right.$$
$$\left.+e_0^2 {l_{in}}^2\frac{\partial^2}{\partial x^2}\left(\rho(x,y)h\frac{\partial v^2}{\partial t^2}\right)+e_0^2 {l_{in}}^2\frac{\partial^2}{\partial y^2}\left(\rho(x,y)h\frac{\partial v^2}{\partial t^2}\right)\right)dxdy=0, \tag{7-b}$$

where, $\psi_u(x,y)$ and $\psi_v(x,y)$ are the arbitrary weight functions. In this paper, we propose a nominal nanoplate by considering the following two conditions. Firstl, the nominal nanoplate is uniformly distributed, e.g. $\overline{Eh}=\frac{E_0 h_0}{A}\iint_A E\left(\frac{x}{a}\right)h\left(\frac{x}{a}\right)dxdy$ and $\overline{\rho h}=\frac{\rho_0 h_0}{A}\iint_A \rho\left(\frac{x}{a}\right)h\left(\frac{x}{a}\right)dxdy$ where A is the surface area of the plate. Secondly, the boundary conditions of the nominal nanoplate contain all the geometric boundary conditions of the non-uniform nanoplate.

The weak form of the FIV for non-uniform nanoplate will be obtained by integrating Eqs. 7. As discussed, the weak form is applied to estimate the solution. To this end, series extensions are used to predict the in-plane displacement of the nanoplate $u(x,y,t)$ and $v(x,y,t)$ as follows:

$$u(x,y,t)=U(x,y)\sin(\omega t) \tag{8-a}$$

$$v(x,y,t)=V(x,y)\sin(\omega t) \tag{8-b}$$

$$\begin{aligned}
&\frac{\overline{Eh}}{1-\nu^2}\left(\psi_u\frac{\partial U}{\partial x}\Big|_A-\iint_A\frac{\partial\psi_u}{\partial x}\frac{\partial U}{\partial x}dxdy\right)+\frac{\nu\overline{Eh}}{1-\nu^2}\left(\psi_u\frac{\partial V}{\partial y}\Big|_A-\iint_A\frac{\partial\psi_u}{\partial x}\frac{\partial V}{\partial y}dxdy\right)\\
&\quad+\frac{\overline{Eh}}{2(1+\nu)}\left(\psi_u\frac{\partial V}{\partial y}\Big|_A-\iint_A\frac{\partial\psi_u}{\partial x}\frac{\partial V}{\partial y}dxdy+\psi_u\frac{\partial U}{\partial y}\Big|_A-\iint_A\frac{\partial\psi_u}{\partial y}\frac{\partial U}{\partial y}dxdy\right)\\
&\quad+\overline{\rho h}\omega^2\left[\iint_A\psi_u U dxdy\right.\\
&\quad\left.-e_0^2{l_{in}}^2\left(\psi_u\frac{\partial U}{\partial x}\Big|_A-\iint_A\frac{\partial\psi_u}{\partial x}\frac{\partial U}{\partial x}dxdy+\psi_u\frac{\partial U}{\partial y}\Big|_A-\iint_A\frac{\partial\psi_u}{\partial y}\frac{\partial U}{\partial y}dxdy\right)\right]=0,
\end{aligned}\tag{9-a}$$

$$\begin{aligned}
&\frac{\overline{Eh}}{1-\nu^2}\left(\psi_v\frac{\partial V}{\partial y}\Big|_A-\iint_A\frac{\partial\psi_v}{\partial y}\frac{\partial V}{\partial y}dxdy\right)+\frac{\nu\overline{Eh}}{1-\nu^2}\left(\psi_v\frac{\partial U}{\partial y}\Big|_A-\iint_A\frac{\partial\psi_v}{\partial x}\frac{\partial U}{\partial y}dxdy\right)\\
&\quad+\frac{\overline{Eh}}{2(1+\nu)}\left(\psi_v\frac{\partial U}{\partial y}\Big|_A-\iint_A\frac{\partial\psi_v}{\partial x}\frac{\partial U}{\partial y}dxdy+\psi_v\frac{\partial V}{\partial x}\Big|_A-\iint_A\frac{\partial\psi_v}{\partial x}\frac{\partial V}{\partial x}dxdy\right)\\
&\quad+\overline{\rho h}\omega^2\left[\iint_A\psi_v V dxdy\right.\\
&\quad\left.-e_0^2{l_{in}}^2\left(\psi_v\frac{\partial V}{\partial x}\Big|_A-\iint_A\frac{\partial\psi_v}{\partial x}\frac{\partial V}{\partial x}dxdy+\psi_v\frac{\partial V}{\partial y}\Big|_A-\iint_A\frac{\partial\psi_v}{\partial y}\frac{\partial V}{\partial y}dxdy\right)\right]=0.
\end{aligned}\tag{9-b}$$

In order to obtain the maximum potential and kinetic energy which are necessary to study the non-uniform nanoplate based on the Ritz method, Eq. (9-a) and Eq. (9-b) are added together neglecting the weight functions for free geometric boundary conditions as shown in Eq. 10.

$$\begin{aligned}
&\int_0^b\int_0^a\overline{\rho h}\omega^2\left[\psi_v V+\psi_u U+e_0^2{l_{in}}^2\left(\frac{\partial\psi_v}{\partial x}\frac{\partial V}{\partial x}+\frac{\partial\psi_v}{\partial y}\frac{\partial V}{\partial y}+\frac{\partial\psi_u}{\partial x}\frac{\partial U}{\partial x}+\frac{\partial\psi_u}{\partial y}\frac{\partial U}{\partial y}\right)\right]dxdy\\
&\quad=\int_0^b\int_0^a\frac{\overline{Eh}}{1-\nu^2}\left[\left(\frac{\partial\psi_v}{\partial y}\frac{\partial V}{\partial y}+\frac{\partial\psi_u}{\partial x}\frac{\partial U}{\partial x}\right)+\nu\left(\frac{\partial\psi_v}{\partial x}\frac{\partial U}{\partial y}+\frac{\partial\psi_u}{\partial x}\frac{\partial V}{\partial y}\right)\right.\\
&\quad\left.+\frac{1-\nu}{2}\left(\frac{\partial\psi_v}{\partial x}\frac{\partial U}{\partial y}+\frac{\partial\psi_v}{\partial x}\frac{\partial V}{\partial x}+\frac{\partial\psi_u}{\partial x}\frac{\partial V}{\partial y}+\frac{\partial\psi_u}{\partial y}\frac{\partial U}{\partial y}\right)\right]dxdy
\end{aligned}\tag{10}$$

With the assumption that $\psi_u(x,y)\cong U(x,y)$ and $\psi_v(x,y)\cong V(x,y)$, Eq. 11 can be obtained.

$$\begin{aligned}
&\omega^2\int_0^b\int_0^a\overline{\rho h}\left[V^2+U^2+e_0^2{l_{in}}^2\left(\left(\frac{\partial V}{\partial x}\right)^2+\left(\frac{\partial V}{\partial y}\right)^2+\left(\frac{\partial U}{\partial x}\right)^2+\left(\frac{\partial U}{\partial y}\right)^2\right)\right]dxdy\\
&\quad=\int_0^b\int_0^a\frac{\overline{Eh}}{1-\nu^2}\left[\left(\frac{\partial V}{\partial y}\right)^2+\left(\frac{\partial U}{\partial x}\right)^2+2\nu\left(\frac{\partial U}{\partial x}\frac{\partial V}{\partial y}\right)+\frac{1-\nu}{2}\left(\frac{\partial V}{\partial x}+\frac{\partial U}{\partial y}\right)^2\right]dxdy
\end{aligned}\tag{11}$$

Due the fact that the Rayleigh-Quotient is expressed as $\omega^2=\frac{U_{max}}{T^*}$, Eq. 11 can be rewritten in terms of $T^*=2T_{max}$ and U_{max} denoting the reference kinetic energy and maximum potential energy of the system respectively. Therefore, the maximum potential and kinetic energies for the non-uniform nanoplate corresponding to the nonlocal theory can be written as follows:

$$U_{max}=\frac{1}{2}\iint_A\frac{\overline{Eh}}{(1-\nu^2)}\left[\left(\frac{\partial U}{\partial x}\right)^2+\left(\frac{\partial V}{\partial y}\right)^2+2\nu\left(\frac{\partial U}{\partial x}\cdot\frac{\partial V}{\partial y}\right)+\frac{(1-\nu)}{2}\left(\frac{\partial U}{\partial y}+\frac{\partial V}{\partial x}\right)^2\right]dxdy,\tag{12-a}$$

$$T_{max}=\frac{1}{2}\iint_A\overline{\rho h}\left[U^2+V^2+e_0^2{l_{in}}^2\left(\left(\frac{\partial U}{\partial x}\right)^2+\left(\frac{\partial U}{\partial y}\right)^2+\left(\frac{\partial V}{\partial x}\right)^2+\left(\frac{\partial V}{\partial y}\right)^2\right)\right]dxdy.\tag{12-b}$$

These equations reduce to the maximum potential and kinetic energy of the local in-plane displacement model assuming $e_0 l_{in} = 0$.

The Rayleigh-Quotient is obtained by equating the maximum potential and kinetic energies as follows:

$$\omega^2 = \frac{\int_0^b \int_0^a \frac{\overline{Eh}}{(1-\nu^2)}\left[\left(\frac{\partial U}{\partial x}\right)^2 + \left(\frac{\partial V}{\partial y}\right)^2 + 2\nu\left(\frac{\partial U}{\partial x}\cdot\frac{\partial V}{\partial y}\right) + \frac{(1-\nu)}{2}\left(\frac{\partial U}{\partial y}+\frac{\partial V}{\partial x}\right)^2\right]dxdy}{\int_0^b \int_0^a \overline{\rho h}\left[U^2 + V^2 + {e_0^2 l_{in}}^2\left(\left(\frac{\partial U}{\partial x}\right)^2 + \left(\frac{\partial U}{\partial y}\right)^2 + \left(\frac{\partial V}{\partial x}\right)^2 + \left(\frac{\partial V}{\partial y}\right)^2\right)\right]dxdy} \tag{13}$$

The following non-dimensional terms for nanoplate are introduced to have generality and ease.

$$X = \frac{x}{a} \quad , \quad Y = \frac{y}{b},$$
$$\overline{Eh} = E_0 h_0 \int_0^1 \int_0^1 E(X)h(X)dXdY \quad , \quad \overline{\rho h} = \rho_0 h_0 \int_0^1 \int_0^1 \rho(X)h(X)dXdY \tag{14}$$

In this study, we assume that the parameters $E(X)$, $\rho(X)$ and $h(X)$ denoting the Young's modulus, density and thickness of the nanoplate vary with X. The varying parameters of the nanoplate are introduced as:

$$m = \rho h = m_0 \rho(X)h(X) = m_0(1 + \delta X + \varpi X^2),$$
$$E(X)h(X) = (1 + \kappa X + \phi X^2), \tag{15}$$

where, δ, ϖ, κ and ϕ are the non-uniformity parameters and m_0 is the mass per unit cross-sectional area of the nanoplate at $X = 0$. The non-dimensional expression for the Rayleigh-Quotient of the nanoplate is given by substituting Eqs. 14 and 15 into Eq. 13. This leads to:

$$\Lambda^{ND} = \frac{\int_0^1 \int_0^1 E(X)h(X)\left[\left(\frac{\partial U}{\partial X}\right)^2 + R^2\left(\frac{\partial V}{\partial Y}\right)^2 + 2\nu R\left(\frac{\partial U}{\partial X}\cdot\frac{\partial V}{\partial Y}\right) + \frac{(1-\nu)}{2}\left(\frac{\partial U}{\partial Y}R + \frac{\partial V}{\partial X}\right)^2\right]dXdY}{\int_0^1 \int_0^1 \rho(X)h(X)\left[U^2 + V^2 + \frac{{e_0^2 l_{in}}^2}{a^2}\left(\left(\frac{\partial U}{\partial X}\right)^2 + \left(\frac{\partial V}{\partial X}\right)^2 + R^2\left(\left(\frac{\partial V}{\partial Y}\right)^2 + \left(\frac{\partial U}{\partial Y}\right)^2\right)\right)\right]dXdY},$$
$$\Lambda^{ND} = \frac{\rho_0 h_0 \omega^2 a^2}{C_{11}^0}, \tag{16}$$

where Λ^{ND} is the non-dimensional frequency parameter of the nanoplate, ρ_0 is the density at $X = 0$, $C_{11}^0 = \frac{E_0 h_0}{1-\nu^2}$ is the extensional stiffness at $X = 0$ and $R = a/b$ denotes the aspect ratio parameter.

We follow the procedure proposed by (Behera and Chakraverty, 2014 [48]) to solve Eq. 16. The following two deflection functions are assumed:

$$U(X,Y) = \sum_{i=1}^{N} C_i^u \phi_i^{(1)}(X,Y),$$
$$V(X,Y) = \sum_{i=1}^{N} C_i^v \phi_i^{(2)}(X,Y). \tag{17}$$

In Eq. 17, C_i^u and C_i^v are the unknown coefficients, N denotes the order of approximation, and $\phi_i^{(1)}$ and $\phi_i^{(2)}$ are the orthonormal admissible shape functions obtained from the Gram-Schmidt process through the following steps:

$$\begin{gathered}\Gamma_i = X^p(1-X)^q Y^r(1-Y)^s \Upsilon_i, \\ \Upsilon_i = \{1, X, Y, X^2, XY, Y^2, X^3, X^2Y, XY^2, Y^3, \dots\}, \\ \phi_1^{(\ )} = \Gamma_1 \quad , \quad \phi_i^{(\ )} = \Gamma_i - \sum_{k=1}^{i-1} \Theta_{ik} \phi_k^{(\ )}, \\ \Theta_{ik} = \frac{\langle \Gamma_i, \phi_k^{(\ )} \rangle}{\langle \phi_k^{(\ )}, \phi_k^{(\ )} \rangle},\end{gathered} \tag{18}$$

where, p, q, r and s represent the edge parameters controlling the boundary conditions at $X = 0$, $X = 1$, $Y = 0$ and $Y = 1$ respectively. Each of the edge parameter can be set to 0, 1 and 2 for free, simply supported and clamped edge conditions respectively. For two-dimensional problems, $\langle a, b \rangle$ indicates the inner product of the two functions $a(X, Y)$ and $b(X, Y)$ defined as:

$$\langle a, b \rangle = \int_0^1 \int_0^1 a(X, Y) b(X, Y) dX dY. \tag{19}$$

The norm of function $\phi_i^{(\ )}(X, Y)$ is expressed using:

$$\left\| \phi_i^{(\ )}(X, Y) \right\| = \sqrt{\int_0^1 \int_0^1 \phi_i^{(\ )}(X, Y)^2 dX dY}, \tag{20}$$

and the normalized shape function, $\bar{\phi}_i^{(\ )}$, can be obtained as $\bar{\phi}_i^{(\ )} = \frac{\phi_i^{(\ )}}{\left\| \phi_i^{(\ )} \right\|}$.

Substituting Eq. 17 into Eq. 16 leads to a generalized eigenvalue problem:

$$[K]\{D\} = \Lambda^{ND}[M]\{D\}, \tag{21}$$

where $[M]$ and $[K]$ are the mass and stiffness matrices and $\{D\} = [C_1^u C_2^u \dots C_N^u \dots C_1^v C_2^v \dots C_N^v]^T$ is the vector of unknowns. The stiffness and mass matrices can be written as:

$$\begin{gathered}K = \begin{bmatrix} K_{11} & K_{12} \\ K_{21} & K_{22} \end{bmatrix}_{2N \times 2N} \\ M = \begin{bmatrix} M_{11} & M_{12} \\ M_{21} & M_{22} \end{bmatrix}_{2N \times 2N}.\end{gathered} \tag{22}$$

One can use the following set of equations to determine the components of stiffness and mass matrices.

$$\begin{gathered}K_{ij}^{11} = \int_0^1 \int_0^1 E(X) \left(\frac{\partial \phi_i^{(1)}}{\partial X} \cdot \frac{\partial \phi_j^{(1)}}{\partial X} + \frac{(1-\nu)}{2} R^2 \frac{\partial \phi_i^{(1)}}{\partial Y} \cdot \frac{\partial \phi_j^{(1)}}{\partial Y} \right) dX dY, \\ K_{ij}^{12} = \int_0^1 \int_0^1 E(X) \left(\nu R \frac{\partial \phi_i^{(1)}}{\partial X} \cdot \frac{\partial \phi_j^{(2)}}{\partial Y} + \frac{(1-\nu)}{2} R \frac{\partial \phi_i^{(1)}}{\partial Y} \cdot \frac{\partial \phi_j^{(2)}}{\partial X} \right) dX dY, \\ K_{ij}^{21} = \int_0^1 \int_0^1 E(X) \left(\nu R \frac{\partial \phi_i^{(2)}}{\partial Y} \cdot \frac{\partial \phi_j^{(1)}}{\partial X} + \frac{(1-\nu)}{2} R \frac{\partial \phi_i^{(2)}}{\partial X} \cdot \frac{\partial \phi_j^{(1)}}{\partial Y} \right) dX dY, \\ K_{ij}^{22} = \int_0^1 \int_0^1 E(X) \left(R^2 \frac{\partial \phi_i^{(2)}}{\partial Y} \cdot \frac{\partial \phi_j^{(2)}}{\partial Y} + \frac{(1-\nu)}{2} \frac{\partial \phi_i^{(2)}}{\partial X} \cdot \frac{\partial \phi_j^{(2)}}{\partial X} \right) dX dY, \\ M_{ij}^{11} = \int_0^1 \int_0^1 \rho(X) h(X) \left[\phi_i^{(1)} \phi_j^{(1)} + \frac{e_0^2 {l_{in}}^2}{a^2} \left(\frac{\partial \phi_i^{(1)}}{\partial X} \cdot \frac{\partial \phi_j^{(1)}}{\partial X} + R^2 \frac{\partial \phi_i^{(1)}}{\partial Y} \cdot \frac{\partial \phi_j^{(1)}}{\partial Y} \right) \right] dX dY, \\ M_{ij}^{12} = M_{ij}^{21} = 0\end{gathered} \tag{23}$$

$$M_{ij}^{22}=\int_0^1\int_0^1\rho(X)h(X)\left[\phi_i^{(2)}\phi_j^{(2)}+\frac{e_0^2{l_{in}}^2}{a^2}\left(\frac{\partial\phi_i^{(2)}}{\partial X}\cdot\frac{\partial\phi_j^{(2)}}{\partial X}+R^2\frac{\partial\phi_i^{(2)}}{\partial Y}\cdot\frac{\partial\phi_j^{(2)}}{\partial Y}\right)\right]dXdY.$$

3. Numerical results and discussions

In this section, the non-dimensional frequency parameters Λ^{ND} have been numerically computed by solving the generalized eigenvalue problem Eq. 21. For computer programming, MAPLE (version 18) is used. Here, the effects of small-scale parameter, non-uniformity parameters, aspect ratio and boundary conditions on the non-dimensional frequency parameter of non-uniform nanoplate have been studied. It should be noted that, hereafter, the scripts F and S are used as to symbolize the Free and Simply supported conditions respectively.

3.1. Validation

For validation purpose, herein, we use an example that was investigated by (Murmu and Pradhan, 2009 [32]) using the method of direct separation variables. To this end, we consider a uniform nanoplate with mass density $\rho=2250\frac{\mathrm{Kg}}{\mathrm{m}^3}$, modulus of elasticity $E=106\,TPa$, thickness $h=0.34$ nm and Poisson's ratio $\nu=0.25$. We take the two lengths of the nanoplate as 5 nm and 30 nm. The nonlocal scale coefficient is assumed to be $e_0l_{in}=0.5,1$ and 2.

Table 1 reports the three non-dimensional frequency ratios $\left(\frac{(\Lambda^{ND})_{nonlocal}}{(\Lambda^{ND})_{local}}\right)$ of the square nanoplate considered above with simply-supported boundary conditions. From Table 1, it can be concluded that the non-dimensional frequency ratio decreases when the nonlocal scale coefficient increases. In addition, when the nonlocal scale coefficient is fixed to a constant value, the non-dimensional frequencies increase with increasing the length of the nanoplate. According to Table 1, the results obtained using the present approach agrees well with those reported in (Murmu and Pradhan, 2009 [32]).

Table 1. Validation of the present result for uniform SSSS nanoplate in different modes

	nm	Mode 1		Mode 2		Mode 5		Mode 20	
		Present	Ref. [31]	Present	Ref. [31]	Present	Ref. [31]	Present	Ref. [31]
$e_0l_{in}=0.5$	L=10	0.9624	0.9762	0.8800	0.9139	0.6352	0.6691	0.1857	0.2196
	L=30	0.9794	0.9973	0.9714	0.9892	0.9199	0.9378	0.5418	0.5596
$e_0l_{in}=1$	L=10	0.8800	0.9139	0.7137	0.7475	0.3766	0.4105	0.0780	0.1118
	L=30	0.9714	0.9892	0.9410	0.9588	0.7858	0.8037	0.3020	0.3199
$e_0l_{in}=2$	L=10	0.7137	0.8475	0.4565	0.4904	0.1857	0.2196	0.0223	0.0562
	L=30	0.9410	0.9588	0.8425	0.8604	0.5418	0.5596	0.1486	0.1665

3.2. Convergence study

The convergence study should be carried out in order to determine the necessary degree of the polynomial set, N, for acceptable results. Figures 2-5 show the convergence of the first three

frequency parameters ($\Omega = \sqrt{\Lambda^{ND}}$) for SSSS, FFFF, SFSF and SSFF nanoplates with aspect ratio $R = 2$ and non-uniformity parameters $\delta = \kappa = \varpi = \phi = 0.1$ respectively. Here, the nonlocal parameter $\gamma = (e_0 l_{in})^2$ is considered as $\gamma = 1$ nm^2 to examine the convergence of results. For a specific material, the corresponding nonlocal parameter γ can be estimated by fitting the results of atomic lattice dynamics or experiment. According to Figs. 2-5, one concludes that the frequency parameters approach to the solutions when the number of terms is taken as N=20.

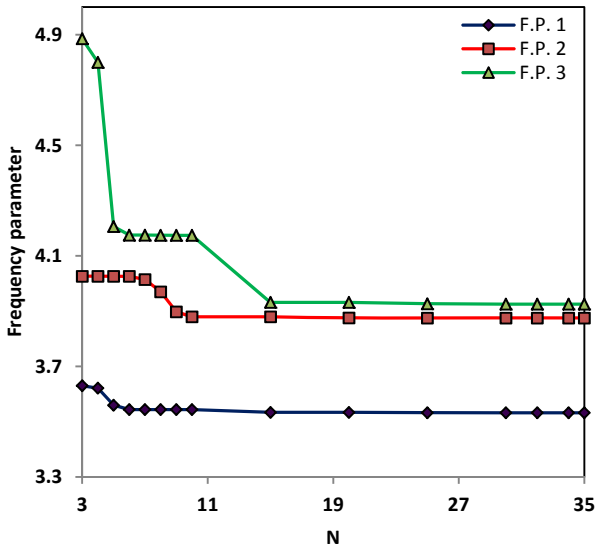

Fig. 2. Convergence of first three frequency parameters for SSSS boundary conditions

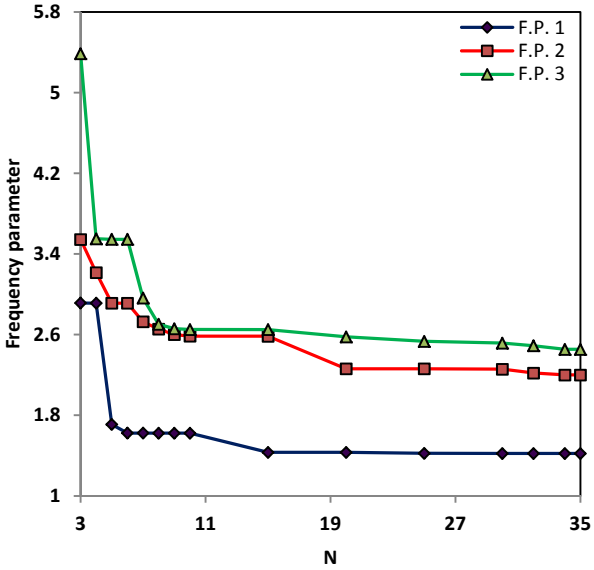

Fig. 3. Convergence of first three frequency parameters for FFFF boundary conditions

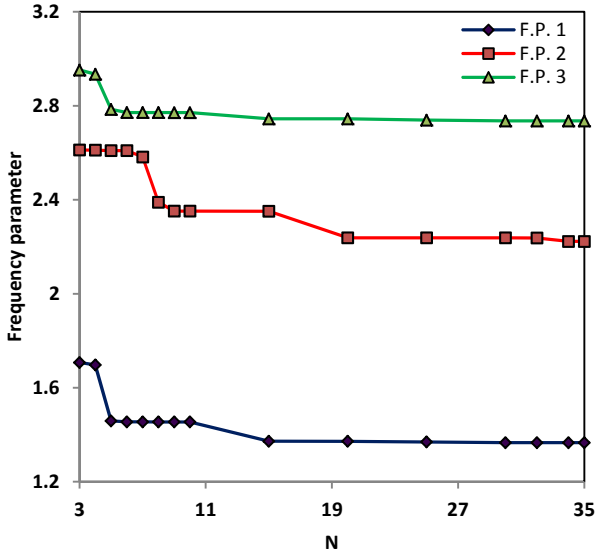

Fig. 4. Convergence of first three frequency parameters for SFSF boundary conditions

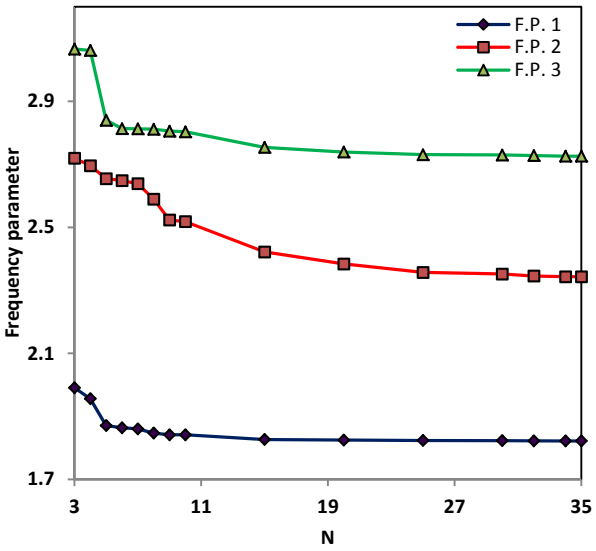

Fig. 5. Convergence of first three frequency parameters for SSFF boundary conditions

3.3. Effect of non-local parameter

The effect of the nonlocal parameter on the frequency parameter is explored in this section. Figure 6 illustrates the variation of the first seven frequency parameters with respect to the nonlocal parameter for FFFF nanoplates with $a = 20$ nm and $R = 5$. The nonlocal parameter is taken as 0 nm^2, 0.5 nm^2, 1 nm^2, 1.5 nm^2, 2 nm^2, 2.5 nm^2, 3 nm^2, 3.5 nm^2, 4 nm^2, 4.5 nm^2 and 5 nm^2. From Fig. 6, it can be seen that the frequency parameter decreases when the nonlocal parameter increases especially at higher modes. Consequently, increasing the nonlocal parameter leads to a reduction in the stiffness of the nanoplate.

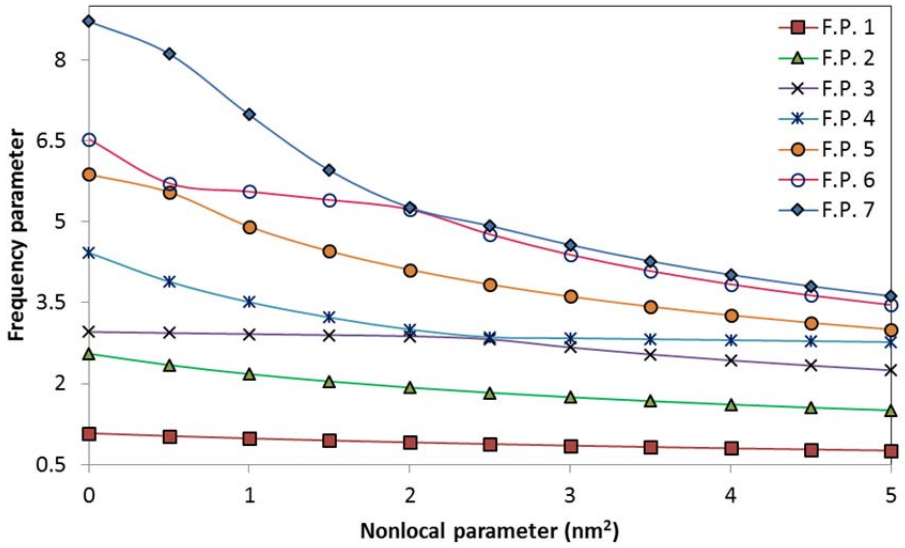

Fig. 6. Variation of the first seven frequency parameters with the nonlocal parameter

Figure 7 demonstrates variation of the first frequency parameter with length for FFFF nanoplates with aspect ratio $R = 4/5$ and non-uniformities $\phi = 0.1$, $\varpi = 0.2$, $\delta = 0.3$ and $\kappa = 0.4$. Here, the nonlocal parameter varies between 0 to 2 nm^2. According to Fig. 7, one can conclude that in a fixed length of nanoplate, the first frequency parameter decreases as the nonlocal parameter increases. Additionally, in a fixed nonlocal parameter, increasing the length of the nanoplate

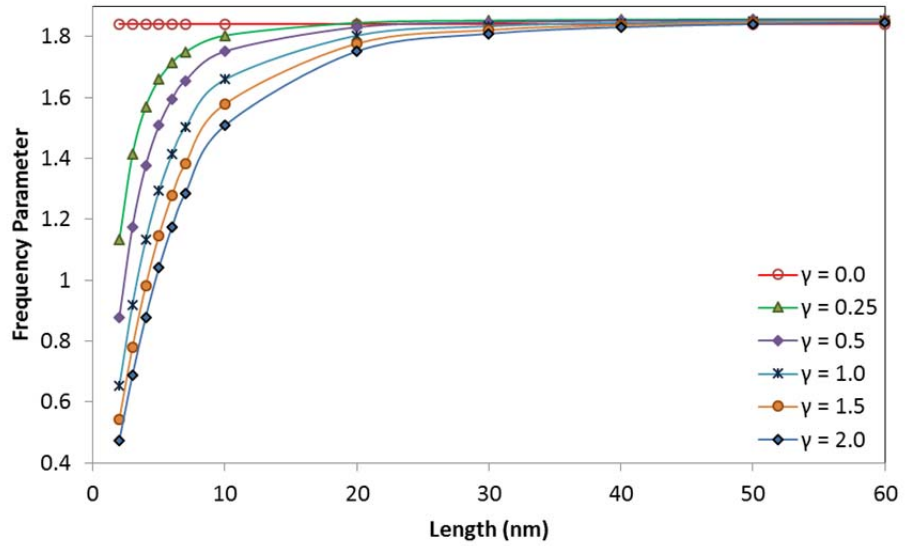

Fig. 7. Variation of the fundamental frequency parameter with length a for different values of γ

causes an increase in the frequency parameter. With this, it becomes clear that in a nanoplate with larger length, the effect of the nonlocal parameter reduces. As a results, as shown in Fig. 7, when the length of a nanoplate is approximately larger than 40 nm, for all nonlocal parameters, the frequency parameter approaches to the local frequency ($\gamma = 0$).

3.4. Effect of non-uniformity parameters

In this part, the effects of non-uniformity parameters on the frequency parameters have been investigated. To this end, first we assume that the mass per unit area and Young's modulus vary quadratically and linearly respectively with $\phi = 0$ and $\delta = 0$. For this example, we take $\gamma = 1\ \text{nm}^2$, $a = 5$ nm and $R = 1$ for the frequency parameters, and ϖ varies from 0.1 to 0.9 with the SFSF edge boundary condition. Figure 8 represents the variation of the first four frequency parameters as functions of ϖ assuming $\kappa = 0.5$. It can be concluded from Fig. 8 that the frequency parameters decrease by increasing ϖ because Λ^{ND} is inversely proportional to ϖ as stated in Eq. 16.

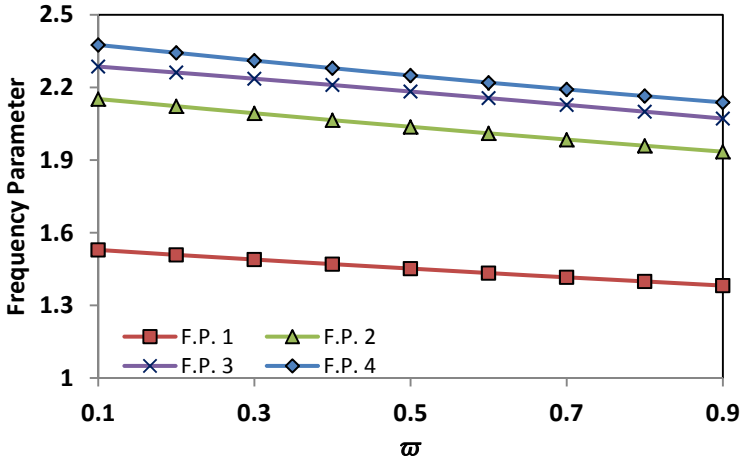

Fig. 8. Variation of the first four frequency parameters with ϖ

Variation of the frequency parameter as function of κ is also investigated and the results are illustrated in Fig. 9. The results are provided assuming that $\gamma = 1\ \text{nm}^2$, $a = 5$ nm and $R = 2$

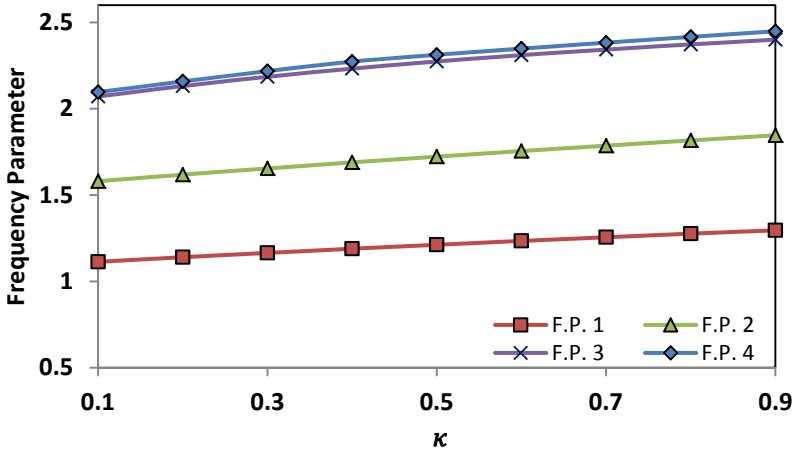

Fig. 9. Variation of the first four frequency parameters with κ

with the SFSF boundary condition taking $\varpi = 0.5$. It is noticed that increasing κ leads to a slight increase in frequency parameters. This behavior was expected; because Λ^{ND} is relatively proportional to κ (see Eq. 16).

Next, we study the effects of non-uniformity parameters on the frequency parameter, when Young's modulus and mass per unit area of the nanoplate vary quadratically by taking $\varpi = 0.2$ and changing ϕ from 0.1 to 0.9. The variation of frequency parameters for this problem assuming the SSSF boundary condition is demonstrated in Fig. 10. Results are determined for $\gamma = 2\,nm^2$, $a = 10\,nm$ and $R = 1$. Results show that frequency parameters increase by increasing ϕ.

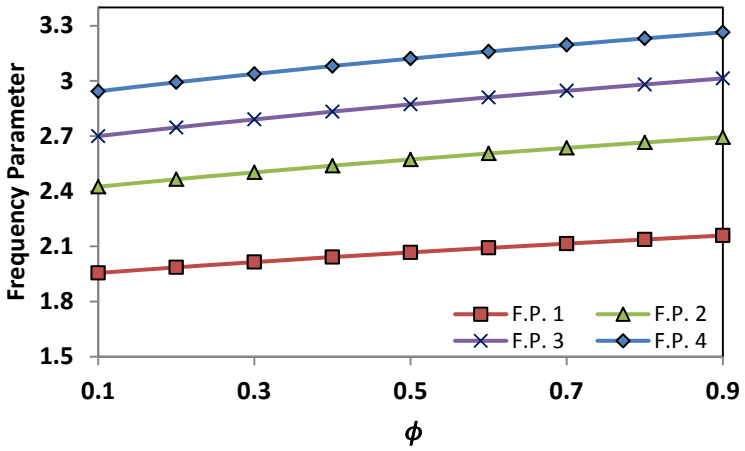

Fig. 10. Variation of the first four frequency parameters with ϕ

Figure 11 represents the alteration of frequency parameters with ϖ taking $\varphi = 0.2$. These frequency parameters are obtained for SSSF boundary condition considering $\gamma = 2\,\mathrm{nm}^2$, $a = 10$ nm and $R = 1$. Results illustrated in Fig. 11 show a reduction in frequency parameters as ϖ increases.

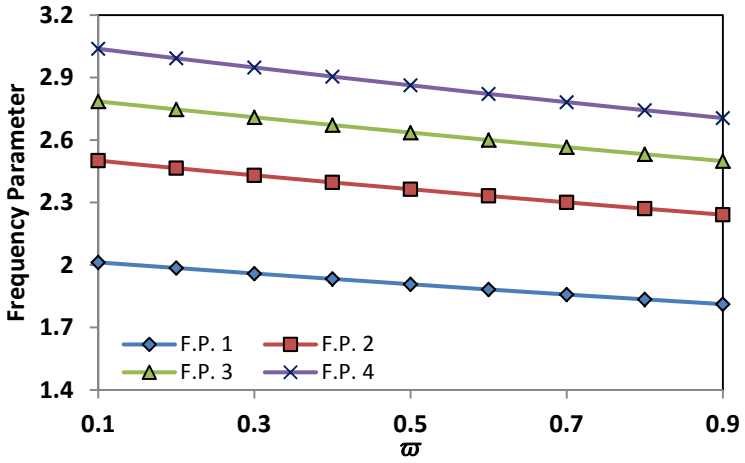

Fig. 11. Variation of the first four frequency parameters with ϖ

In the last attempt, we investigate the effects of non-uniformity parameter on frequency parameters for the case where Young's modulus varies quadratically and the mass per unit area varies linearly. This case study can be obtained by taking $\kappa = 0$ and $\varpi = 0$. The variations of the first four frequency parameters with δ is demonstrated in Fig. 12 for the case of SSSF for boundary condition taking $\varphi = 0.2$. These solutions again are provided for $\gamma = 2\,\mathrm{nm}^2$, $a = 10\,\mathrm{nm}$ and $R = 1$. According to Fig. 12, one can conclude that frequency parameters decrease with increase in δ.

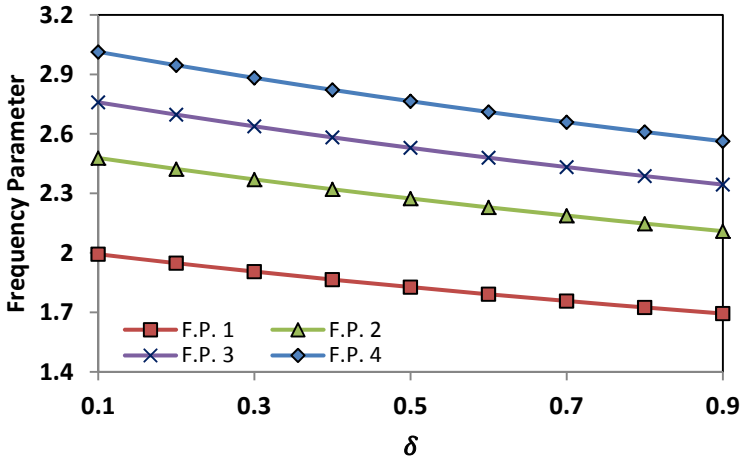

Fig. 12. Variation of the first four frequency parameters with δ

3.5. Effect of aspect ratio parameter

In this section we aim to constrain the influence of the aspect ratio on the FIV of the non-uniform nanoplates. To this end, the fundamental frequency parameter is depicted for various aspect ratios in Fig. 13 for the case of SSSS boundary condition with $a = 10\,\mathrm{nm}$, $\kappa = 1$, $\phi = \delta = 3$ and $\varpi = 2$. From Fig. 13, it is noticed that the fundamental frequency is more affected by nonlocal parameter at high aspect ratio. However, for all nonlocal parameters, increasing aspect ratio leads to an increase in the fundamental frequency because in a fixed width, aspect ratio

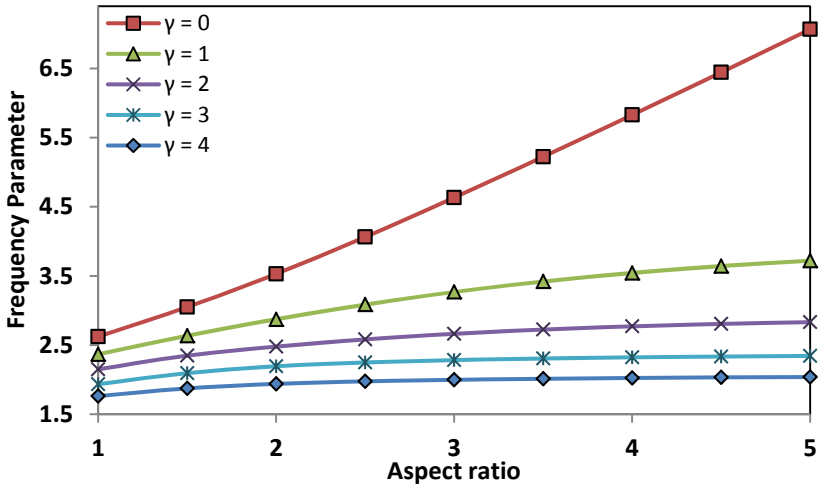

Fig. 13. Variation of the fundamental frequency parameter with aspect ratio for different values of γ

directly represents the length of the nanoplate (see section 2), i.e. increasing the aspect ratio is equivalent to increasing the length of the nanoplate. Furthermore, at a fixed aspect ratio, by increasing the nonlocal parameter, the fundamental frequency is decreased which implies that the nonlocal effects should be taken into consideration in FIV of nanoplates at high aspect ratios.

3.6. Effect of boundary conditions

In this subsection, the influence of boundary conditions on the frequency parameter is investigated. Proper information about the effect of boundary conditions on frequency parameter is necessary to better design nano-structures. The variation of the fundamental frequency parameter with small-scale effect is shown in Fig. 14 for all combinations of boundary conditions with $a = 10$ nm, $\kappa = 0.4$, $\delta = 0.3$, $\phi = 0.2$, $\varpi = 0.1$ and $R = 1$. As shown in Fig. 14, the fundamental frequency parameter decreases with increase in nonlocal parameter which varies between 0 to 2 nm. It is also detected from Fig. 14 that SSSS and SFFF nanoplates possess the highest and lowest frequency parameters respectively. Additionally, increasing the small-scale effect has a maximum and minimum effect on the fundamental frequency parameter when the boundary conditions of nanoplate are SSSS and SFFF respectively.

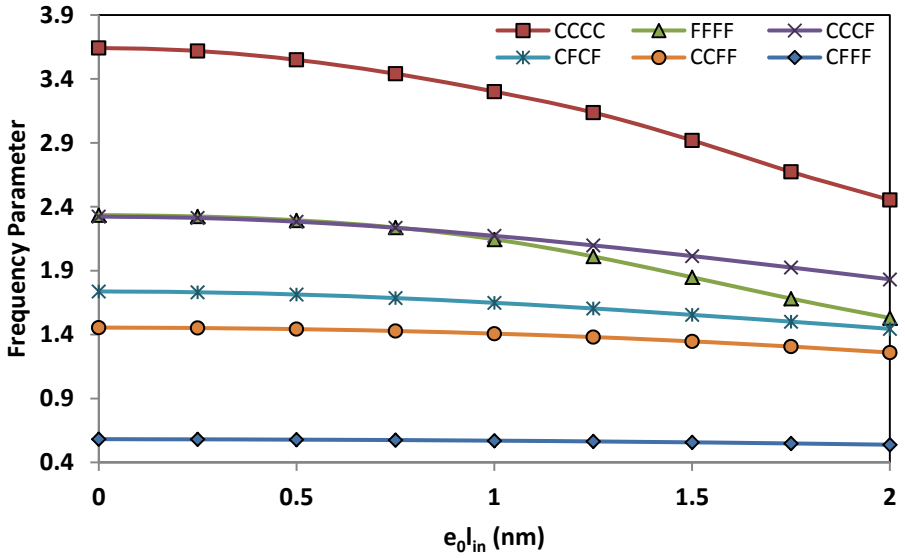

Fig. 14. Variation of the fundamental frequency parameter with the nonlocal scale coefficient for different boundary conditions

3.7. Mode shapes

Lastly, we explore the influence of the nonlocal scale coefficient on mode shapes because knowing the mode shapes of engineering structures is necessary for design purposes. For this

aim, the second, sixth and twelfth mode shapes of a SFSF nanoplate is provided for different values of $e_0 l_{in}$ varying from zero to three and non-uniform parameters are selected such that $\kappa = 0.4$, $\delta = 0.3$, $\phi = 0.2$, $\varpi = 0.1$, $a = 5$ nm and $R = 1$. The results are shown in Fig. 15 that shows mode shapes are influenced by scaling effect parameter. The non-local continuum model has an atomistic view in which the atoms are connected by elastic springs, while for the local (classic) continuum model, the spring constants have infinitive values. In a specific mode, when the scale coefficient $e_0 l_{in}$ increases from zero to three, the stiffness of the system decreases, the system becomes softer with lower frequency and behaves like a *new* discrete lumped mass-spring system. Therefore, for the new system, a new qualitative dynamical behavior is expected and a new set of *small-waves* appears in the mode-shapes due to considering the interatomic spacing in the analysis that leads to atoms fluctuations during wave propagation phenomenon.

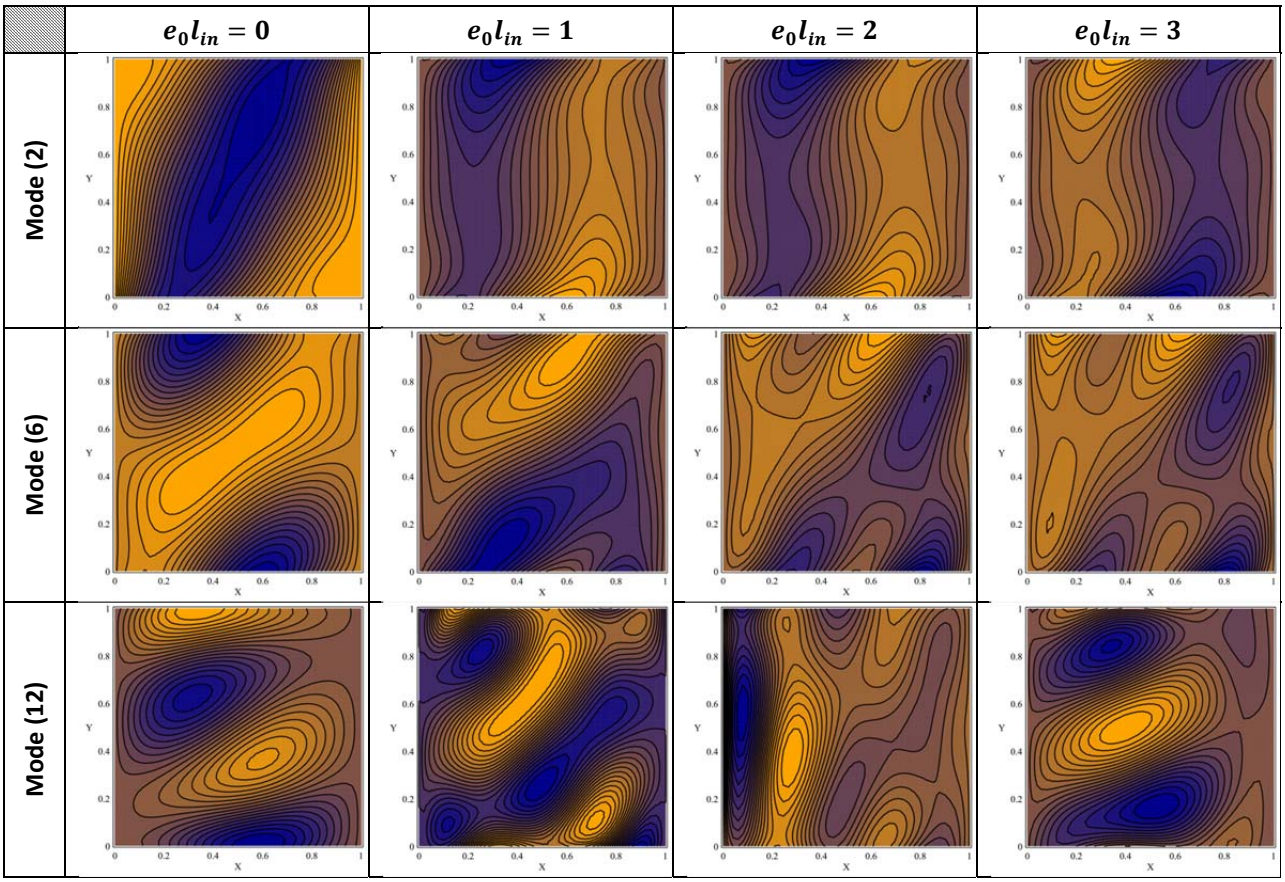

Fig. 15. 2nd, 6th and 12th mode-shapes of a non-uniform SFSF nanoplate with different values of nonlocal scale coefficient

4. Conclusions

In this paper, the effect of non-uniformity parameters on in-plane frequency parameters of nanoplates is studied using a numerically efficient method. This method employs the boundary characteristic orthogonal polynomials produced using the Gram–Schmidt process and is based on the Ritz method. The non-uniformity of the nanoplates is applied assuming linear and quadratic variations of Young's modulus and density. A convergence study is carried out for a specific set of parameters to show the accuracy of the present method. The obtained solutions have been tested against the existing results for simply supported edge conditions and satisfactory agreement was observed. We provided a comprehensive study of the effect of non-uniform parameter, nonlocal parameter, small-scale, aspect ratio and boundary conditions on the in-plane frequency parameters. The main obtained results from this work can be itemized as:

Frequency parameters decrease by increasing the nonlocal parameter in all the vibration modes.

Frequency parameters decrease by increasing ϖ and δ, and increase by increasing ϕ and κ.

Frequency parameters increase by increasing the aspect ratio for different values of nonlocal parameters.

The small-scale effect has more influence on frequency parameters at higher values of aspect ratio.

Finally, mode shapes are considerably affected by scaling effect parameters.

From these results, the importance of the nonlocal elasticity theory is highlighted. The nonlocal elasticity must be taken into consideration for the FIV of nanoplates because the classical (local) plate model generally overestimates the in-plane frequency.

References

[1] S. Thomas, N. Kalarikkal, A. Manuel Stephan, B. Raneesh, A.K. Haghi, Advanced nanomaterials: Synthesis, properties, and applications, Apple Academic Press, 2014.
[2] T. Murmu, S. Adhikari, Nonlocal transverse vibration of double-nanobeam-systems, Journal of Applied Physics, 108 (2010) 083514.
[3] F. Baletto, R. Ferrando, Structural properties of nanoclusters: Energetic, thermodynamic, and kinetic effects, Reviews of Modern Physics, 77 (2005) 371-423.
[4] A.S. Afolabi, A.S. Abdulkareem, S.E. Iyuke, H.C. Van Zyl Pienaar, Continuous production of carbon nanotubes and diamond films by swirled floating catalyst chemical vapour deposition method, South African Journal of Science, 105 (2009) 278-281.
[5] K. Nagashio, T. Nishimura, K. Kita, A. Toriumi, Mobility variations in mono-and multi-layer graphene films, Applied Physics Express (APEX), 2 (2009) 025003.
[6] A.I. Gusev, A.A. Rempel, Nanocrystalline Materials, Cambridge International Science Publishing, Cambridge, U.K., 2004.
[7] X. Li, W. Liu, L. Sun, K.E. Aifantis, B. Yu, Y. Fan, Q. Feng, F. Cui, F. Watari, Effects of physicochemical properties of nanomaterials on their toxicity, Journal of Biomedical Materials Research Part A, 103 (2015) 2499-2507.

[8] I. Favero, S. Stapfner, D. Hunger, P. Paulitschke, J. Reichel, H. Lorenz, E.M. Weig, K. Karrai, Fluctuating nanomechanical system in a high finesse optical microcavity, Optics express, 17 (2009) 12813-12820.
[9] M. Poot, H.S.J. Van der Zant, Nanomechanical properties of few-layer graphene membranes, Applied Physics Letters, 92 (2008) 063111.
[10] P. Ball, Roll up for the revolution, Nature, 414 (2001) 142-144.
[11] R.H. Baughman, A.A. Zakhidov, W.A. De Heer, Carbon nanotubes: The route toward applications, Science, 297 (2002) 787-792.
[12] B.H. Bodily, C.T. Sun, Structural and equivalent continuum properties of single-walled carbon nanotubes, International Journal of Materials and Product Technology, 18 (2003) 381-397.
[13] C. Li, T.W. Chou, A structural mechanics approach for the analysis of carbon nanotubes, International Journal of Solids and Structures, 40 (2003) 2487-2499.
[14] R. Liu, L. Wang, Thermal vibration of a single-walled carbon nanotube predicted by semiquantum molecular dynamics, Physical Chemistry Chemical Physics, 17 (2015) 5194-5201.
[15] C. Li, T.W. Chou, Quantized molecular structural mechanics modeling for studying the specific heat of single-walled carbon nanotubes, Physical Review B, 71 (2005) 075409.
[16] T. Yumura, A density functional theory study of chemical functionalization of carbon nanotubes; Toward site selective functionalization, INTECH Open Access Publisher, 2011.
[17] S. Adali, Variational principles for nonlocal continuum model of orthotropic graphene sheets embedded in an elastic medium, Acta Mathematica Scientia, 32 (2012) 325-338.
[18] M.R. Karamooz Ravari, A.R. Shahidi, Axisymmetric buckling of the circular annular nanoplates using finite difference method, Meccanica, 48 (2013) 135-144.
[19] P. Lu, H.P. Lee, C. Lu, P.Q. Zhang, Dynamic properties of flexural beams using a nonlocal elasticity model, Journal of Applied Physics, 99 (2006) 073510.
[20] H.S. Shen, Nonlocal plate model for nonlinear analysis of thin films on elastic foundations in thermal environments, Composite Structures, 93 (2011) 1143-1152.
[21] C.Y. Wang, T. Murmu, S. Adhikari, Mechanisms of nonlocal effect on the vibration of nanoplates, Applied Physics Letters, 98 (2011) 153101.
[22] A.C. Eringen, Linear theory of nonlocal elasticity and dispersion of plane waves, International Journal of Engineering Science, 10 (1972) 425-435.
[23] A.C. Eringen, On differential equations of nonlocal elasticity and solutions of screw dislocation and surface waves, Journal of Applied Physics, 54 (1983) 4703-4710.
[24] A.C. Eringen, Nonlocal continuum field theories, Springer Science & Business Media, 2002.
[25] T.P. Chang, Small scale effect on axial vibration of non-uniform and non-homogeneous nanorods, Computational Materials Science, 54 (2012) 23-27.
[26] Loya, J. López-Puente, R. Zaera, J. Fernández-Sáez, Free transverse vibrations of cracked nanobeams using a nonlocal elasticity model, Journal of Applied Physics, 105 (2009) 044309.
[27] T. Aksencer, M. Aydogdu, Levy type solution method for vibration and buckling of nanoplates using nonlocal elasticity theory, Physica E: Low-dimensional Systems and Nanostructures, 43 (2011) 954-959.
[28] A. Anjomshoa, Application of Ritz functions in buckling analysis of embedded orthotropic circular and elliptical micro/nano-plates based on nonlocal elasticity theory, Meccanica, 48 (2013) 1337-1353.

[29] Y.G. Hu, K.M. Liew, Q. Wang, X.Q. He, B.I. Yakobson, Nonlocal shell model for elastic wave propagation in single-and double-walled carbon nanotubes, Journal of the Mechanics and Physics of Solids, 56 (2008) 3475-3485.
[30] N.P. Bansal, J. Lamon, Ceramic matrix composites: Materials, modeling and technology, John Wiley & Sons, 2014.
[31] V. Yantchev, I. Katardjiev, Thin film Lamb wave resonators in frequency control and sensing applications: a review, Journal of Micromechanics and Microengineering, 23 (2013) 043001.
[32] T. Murmu, S.C. Pradhan, Small-scale effect on the free in-plane vibration of nanoplates by nonlocal continuum model, Physica E: Low-dimensional Systems and Nanostructures, 41 (2009) 1628-1633.
[33] J. Cumings, P.G. Collins, A. Zettl, Peeling and sharpening multiwall nanotubes, Nature, 406 (2000) 586.
[34] A.M. Brodsky, Control of phase transition dynamics in media with nanoscale nonuniformities by coherence loss spectroscopy, Journal of Optics, 12 (2010) 095702.
[35] S. Chakraverty, L. Behera, Free vibration of non-uniform nanobeams using Rayleigh–Ritz method, Physica E: Low-dimensional Systems and Nanostructures, 67 (2015) 38-46.
[36] A. Koochi, H.M. Sedighi, M. Abadyan, Modeling the size dependent pull-in instability of beam-type NEMS using strain gradient theory, Latin American Journal of Solids and Structures, 11 (2014) 1806-1829.
[37] X.J. Xu, Z.C. Deng, Variational principles for buckling and vibration of MWCNTs modeled by strain gradient theory, Applied Mathematics and Mechanics, 35 (2014) 1115-1128.
[38] S. Chakraverty, L. Behera, Free vibration of rectangular nanoplates using Rayleigh–Ritz method, Physica E: Low-dimensional Systems and Nanostructures, 56 (2014) 357-363.
[39] R.B. Bhat, Plate deflections using orthogonal polynomials, Journal of Engineering Mechanics, 111 (1985) 1301-1309.
[40] R.B. Bhat, Vibration of rectangular plates on point and line supports using characteristic orthogonal polynomials in the Rayleigh-Ritz method, Journal of sound and vibration, 149 (1991) 170-172.
[41] T.S. Chihara, An introduction to orthogonal polynomials, Gordon and Breach, Science Publisher, Inc., New York, 1978.
[42] S.M. Dickinson, A. Di Blasio, On the use of orthogonal polynomials in the Rayleigh-Ritz method for the study of the flexural vibration and buckling of isotropic and orthotropic rectangular plates, Journal of Sound and Vibration, 108 (1986) 51-62.
[43] W. Gautschi, G.H. Golub, G. Opfer, Applications and computation of orthogonal polynomials, ADVANCES IN, (1999) 251.
[44] B. Singh, S. Chakraverty, Boundary characteristic orthogonal polynomials in numerical approximation, Communications in Numerical Methods in Engineering, 10 (1994) 1027-1043.
[45] B. Singh, S. Chakraverty, Use of characteristic orthogonal polynomials in two dimensions for transverse vibration of elliptic and circular plates with variable thickness, Journal of Sound and Vibration, 173 (1994) 289-299.
[46] P. Lu, P.Q. Zhang, H.P. Lee, C.M. Wang, J.N. Reddy, Non-local elastic plate theories, in: Proceedings of the Royal Society of London A: Mathematical, Physical and Engineering Sciences, The Royal Society, 2007, pp. 3225-3240.
[47] D.J. Gorman, Free in-plane vibration analysis of rectangular plates by the method of superposition, Journal of Sound and Vibration, 272 (2004) 831-851.

[48] L. Behera, S. Chakraverty, Free vibration of Euler and Timoshenko nanobeams using boundary characteristic orthogonal polynomials, Applied Nanoscience, 4 (2014) 347-358.